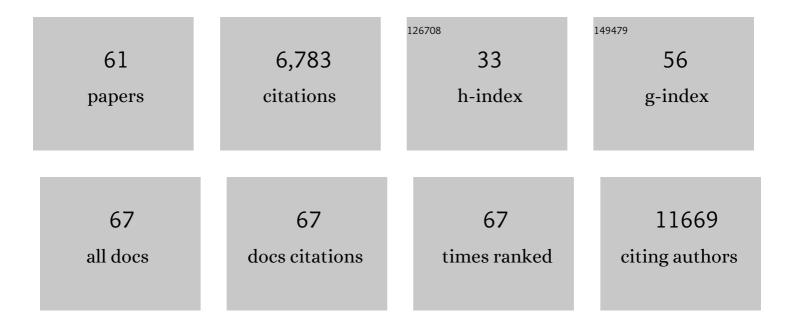
Haydyn D T Mertens

List of Publications by Year in descending order

Source: https://exaly.com/author-pdf/5107510/publications.pdf Version: 2024-02-01



#	Article	IF	CITATIONS
1	New developments in the <i>ATSAS</i> program package for small-angle scattering data analysis. Journal of Applied Crystallography, 2012, 45, 342-350.	1.9	1,551
2	<i>ATSAS 2.8</i> : a comprehensive data analysis suite for small-angle scattering from macromolecular solutions. Journal of Applied Crystallography, 2017, 50, 1212-1225.	1.9	1,205
3	Advanced ensemble modelling of flexible macromolecules using X-ray solution scattering. IUCrJ, 2015, 2, 207-217.	1.0	516
4	<i>ATSAS 3.0</i> : expanded functionality and new tools for small-angle scattering data analysis. Journal of Applied Crystallography, 2021, 54, 343-355.	1.9	512
5	Structural characterization of proteins and complexes using small-angle X-ray solution scattering. Journal of Structural Biology, 2010, 172, 128-141.	1.3	470
6	A low-background-intensity focusing small-angle X-ray scattering undulator beamline. Journal of Applied Crystallography, 2013, 46, 1670-1680.	1.9	450
7	Structural basis for engagement by complement factor H of C3b on a self surface. Nature Structural and Molecular Biology, 2011, 18, 463-470.	3.6	220
8	The Crystal Structure of Netrin-1 in Complex with DCC Reveals the Bifunctionality of Netrin-1 As a Guidance Cue. Neuron, 2014, 83, 839-849.	3.8	103
9	Structure of the mycobacterial ESX-5 type VII secretion system membrane complex by single-particle analysis. Nature Microbiology, 2017, 2, 17047.	5.9	102
10	Ammonium hydroxide treatment of AÎ ² produces an aggregate free solution suitable for biophysical and cell culture characterization. PeerJ, 2013, 1, e73.	0.9	93
11	Saposin Lipid Nanoparticles: A Highly Versatile and Modular Tool for Membrane Protein Research. Structure, 2018, 26, 345-355.e5.	1.6	69
12	The PHD and Chromo Domains Regulate the ATPase Activity of the Human Chromatin Remodeler CHD4. Journal of Molecular Biology, 2012, 422, 3-17.	2.0	68
13	Stabilization of Nontoxic AÂ-Oligomers: Insights into the Mechanism of Action of Hydroxyquinolines in Alzheimer's Disease. Journal of Neuroscience, 2015, 35, 2871-2884.	1.7	67
14	Structure of the lipoprotein lipase–GPIHBP1 complex that mediates plasma triglyceride hydrolysis. Proceedings of the National Academy of Sciences of the United States of America, 2019, 116, 1723-1732.	3.3	67
15	Structure, topology and function of the translocase of the outer membrane of mitochondria. Plant Physiology and Biochemistry, 2008, 46, 265-274.	2.8	59
16	Cell-free protein synthesis of membrane (1,3)-β-d-glucan (curdlan) synthase: Co-translational insertion in liposomes and reconstitution in nanodiscs. Biochimica Et Biophysica Acta - Biomembranes, 2013, 1828, 743-757.	1.4	58
17	Conformational States of ABC Transporter MsbA in a Lipid Environment Investigated by Small-Angle Scattering Using Stealth Carrier Nanodiscs. Structure, 2018, 26, 1072-1079.e4.	1.6	58
18	Structure, Function, and Biosynthetic Origin of Octapeptin Antibiotics Active against Extensively Drug-Resistant Gram-Negative Bacteria. Cell Chemical Biology, 2018, 25, 380-391.e5.	2.5	57

HAYDYN D T MERTENS

#	Article	IF	CITATIONS
19	Unfolding of monomeric lipoprotein lipase by ANGPTL4: Insight into the regulation of plasma triglyceride metabolism. Proceedings of the National Academy of Sciences of the United States of America, 2020, 117, 4337-4346.	3.3	56
20	A Structural Core Within Apolipoprotein C-II Amyloid Fibrils Identified Using Hydrogen Exchange and Proteolysis. Journal of Molecular Biology, 2007, 366, 1639-1651.	2.0	53
21	The Central Portion of Factor H (Modules 10–15) Is Compact and Contains a Structurally Deviant CCP Module. Journal of Molecular Biology, 2010, 395, 105-122.	2.0	51
22	Epsin and Sla2 form assemblies through phospholipid interfaces. Nature Communications, 2018, 9, 328.	5.8	47
23	Combining NMR and small angle X-ray scattering for the study of biomolecular structure and dynamics. Archives of Biochemistry and Biophysics, 2017, 628, 33-41.	1.4	46
24	Characterisation of the First Enzymes Committed to Lysine Biosynthesis in Arabidopsis thaliana. PLoS ONE, 2012, 7, e40318.	1.1	45
25	LabDisk for SAXS: a centrifugal microfluidic sample preparation platform for small-angle X-ray scattering. Lab on A Chip, 2016, 16, 1161-1170.	3.1	44
26	Recognition of Mitochondrial Targeting Sequences by the Import Receptors Tom20 and Tom22. Journal of Molecular Biology, 2011, 405, 804-818.	2.0	43
27	A Flexible Multidomain Structure Drives the Function of the Urokinase-type Plasminogen Activator Receptor (uPAR)*. Journal of Biological Chemistry, 2012, 287, 34304-34315.	1.6	43
28	Structural Analysis of the C-Terminal Region (Modules 18–20) of Complement Regulator Factor H (FH). PLoS ONE, 2012, 7, e32187.	1.1	39
29	Structural Basis for Draxin-Modulated Axon Guidance and Fasciculation by Netrin-1 through DCC. Neuron, 2018, 97, 1261-1267.e4.	3.8	39
30	The CD27L and CTP1L Endolysins Targeting Clostridia Contain a Built-in Trigger and Release Factor. PLoS Pathogens, 2014, 10, e1004228.	2.1	37
31	Crystal Structure of the CTP1L Endolysin Reveals How Its Activity Is Regulated by a Secondary Translation Product. Journal of Biological Chemistry, 2016, 291, 4882-4893.	1.6	36
32	Signaling ammonium across membranes through an ammonium sensor histidine kinase. Nature Communications, 2018, 9, 164.	5.8	36
33	Structural Model of the Cytosolic Domain of the Plant Ethylene Receptor 1 (ETR1). Journal of Biological Chemistry, 2015, 290, 2644-2658.	1.6	35
34	Small Oligomers of Ribulose-bisphosphate Carboxylase/Oxygenase (Rubisco) Activase Are Required for Biological Activity. Journal of Biological Chemistry, 2013, 288, 20607-20615.	1.6	30
35	Using Mutagenesis and Structural Biology to Map the Binding Site for the Plasmodium falciparum Merozoite Protein PfRh4 on the Human Immune Adherence Receptor. Journal of Biological Chemistry, 2014, 289, 450-463.	1.6	30
36	Structural basis for activation of plasma-membrane Ca2+-ATPase by calmodulin. Communications Biology, 2018, 1, 206.	2.0	30

HAYDYN D T MERTENS

#	Article	IF	CITATIONS
37	A Barley Efflux Transporter Operates in a Na ⁺ -Dependent Manner, as Revealed by a Multidisciplinary Platform. Plant Cell, 2016, 28, 202-218.	3.1	29
38	Lack of Evidence from Studies of Soluble Protein Fragments that Knops Blood Group Polymorphisms in Complement Receptor-Type 1 Are Driven by Malaria. PLoS ONE, 2012, 7, e34820.	1.1	25
39	Small angle X-ray scattering analysis of Cu2+-induced oligomers of the Alzheimer's amyloid β peptide. Metallomics, 2015, 7, 536-543.	1.0	25
40	Solution Structure of CCP Modules 10–12 Illuminates Functional Architecture of the Complement Regulator, Factor H. Journal of Molecular Biology, 2012, 424, 295-312.	2.0	24
41	Alpha-synuclein oligomers and fibrils originate in two distinct conformer pools: a small angle X-ray scattering and ensemble optimisation modelling study. Molecular BioSystems, 2015, 11, 190-196.	2.9	24
42	From Knock-Out Phenotype to Three-Dimensional Structure of a Promising Antibiotic Target from Streptococcus pneumoniae. PLoS ONE, 2013, 8, e83419.	1.1	22
43	Death-Associated Protein Kinase Activity Is Regulated by Coupled Calcium/Calmodulin Binding to Two Distinct Sites. Structure, 2016, 24, 851-861.	1.6	21
44	Conformational Analysis of a Genetically Encoded FRET Biosensor byÂSAXS. Biophysical Journal, 2012, 102, 2866-2875.	0.2	19
45	Restoring structural parameters of lipid mixtures from small-angle X-ray scattering data. Journal of Applied Crystallography, 2021, 54, 169-179.	1.9	17
46	Structural Insights into the Polyphyletic Origins of Glycyl tRNA Synthetases. Journal of Biological Chemistry, 2016, 291, 14430-14446.	1.6	16
47	Structural model of human dUTPase in complex with a novel proteinaceous inhibitor. Scientific Reports, 2018, 8, 4326.	1.6	15
48	Structure of full-length wild-type human phenylalanine hydroxylase by small angle X-ray scattering reveals substrate-induced conformational stability. Scientific Reports, 2019, 9, 13615.	1.6	13
49	Structure of the endocytic adaptor complex reveals the basis for efficient membrane anchoring during clathrin-mediated endocytosis. Nature Communications, 2021, 12, 2889.	5.8	13
50	An automated data processing and analysis pipeline for transmembrane proteins in detergent solutions. Scientific Reports, 2020, 10, 8081.	1.6	12
51	Did evolution create a flexible ligand-binding cavity in the urokinase receptor through deletion of a plesiotypic disulfide bond?. Journal of Biological Chemistry, 2019, 294, 7403-7418.	1.6	11
52	Structural role of essential light chains in the apicomplexan glideosome. Communications Biology, 2020, 3, 568.	2.0	10
53	Measuring the Molecular Dimensions of Wine Tannins: Comparison of Small-Angle X-ray Scattering, Gel-Permeation Chromatography and Mean Degree of Polymerization. Journal of Agricultural and Food Chemistry, 2014, 62, 7216-7224.	2.4	5
54	Conformational flexibility of EptA driven by an interdomain helix provides insights for enzyme–substrate recognition. IUCrJ, 2021, 8, 732-746.	1.0	5

HAYDYN D T MERTENS

#	Article	IF	CITATIONS
55	Impact of Fluorinated Ionic Liquids on Human Phenylalanine Hydroxylase—A Potential Drug Delivery System. Nanomaterials, 2022, 12, 893.	1.9	5
56	N-terminal phosphorylation regulates the activity of glycogen synthase kinase 3 from <i>Plasmodium falciparum</i> . Biochemical Journal, 2022, 479, 337-356.	1.7	2
57	Hybrid solution methods for tackling membrane proteins. Acta Crystallographica Section A: Foundations and Advances, 2017, 73, a66-a66.	0.0	0
58	Outrunning radiation damage in synchrotron biological small-angle X-ray scattering. Acta Crystallographica Section A: Foundations and Advances, 2017, 73, a191-a191.	0.0	0
59	Integrating SEC-SAXS with MALLS/QELS/RI at the EMBL-P12 bioSAXS beamline. Acta Crystallographica Section A: Foundations and Advances, 2017, 73, C652-C652.	0.0	Ο
60	ATSAS 2.8 software for small-angle scattering from macromolecular solutions. Acta Crystallographica Section A: Foundations and Advances, 2017, 73, C647-C647.	0.0	0
61	Coflow SEC-SAXS at high flux. Acta Crystallographica Section A: Foundations and Advances, 2018, 74, a336-a336.	0.0	0